Influence of the Fe-Co ratio on the exchange coupling in TbFeCo/[Co/Pt] heterostructures

B. Hebler,[1] S. Böttger,[2] D. Nissen,[1] R. Abrudan,[3,4] F. Radu,[3] and M. Albrecht[1]
[1]*Institute of Physics, University of Augsburg, Universitätsstraße 1, D-86159 Augsburg, Germany*
[2]*Institute of Physics, Technische Universität Chemnitz, Reichenhainer Straße 70, D-09126 Chemnitz, Germany*
[3]*Helmholtz-Zentrum Berlin (HZB) für Materialien und Energie, BESSY II, Albert-Einstein-Straße 15, D-12489 Berlin, Germany*
[4]*Institute for Condensed Matter Physics, Ruhr-Universität Bochum, D-44780 Bochum, Germany*
(Received 3 March 2016; revised manuscript received 18 April 2016; published 18 May 2016)

We report on a systematic study of exchange coupled heterostructures, consisting of ferromagnetic [Co/Pt] multilayers and ferrimagnetic (FI) $Tb_xFe_{100-x-y}Co_y$ (20 nm) alloy thin films with varying composition exhibiting strong perpendicular magnetic anisotropy. In particular, the impact of the Tb content and ratio of Fe and Co of the amorphous FI alloy on the exchange interaction at the interface was investigated. In this paper, the magnetic properties of single ternary TbFeCo thin films were analyzed in a broad composition range and compared to coupled TbFeCo/[Co/Pt] heterostructures. While a rather linear dependence of the exchange coupling strength was observed for Fe/Co-dominated ferrimagnets with increasing amount of Co, a nonlinear behavior is observed for Tb-dominated alloys. The latter behavior is governed by the variation of the exchange stiffness of the ferrimagnet. Additionally, by using element-specific x-ray magnetic circular dichroism measurements, the thickness of the interface domain wall (IDW) in the ferrimagnet, which is formed during the reversal of the ferromagnet, can be extracted. An inverse correlation between the IDW thickness and the exchange coupling strength at the interface was deduced.

DOI: 10.1103/PhysRevB.93.184423

I. INTRODUCTION

Exchange coupling phenomena, especially the exchange bias effect of coupled heterostructures consisting of antiferromagnetic (AFM) and ferromagnetic (FM) layers, have been investigated intensively for 60 years [1–8]. The realization of a large exchange bias field is an important aspect in the miniaturization of prospective spintronic devices [2]. Therefore, it is necessary to understand all aspects, which will maximize this effect. However, typical AFM/FM systems show a limitation in achieving large exchange bias fields, which relates to difficulties in controlling the AFM domain state and the uncompensated spin moments at the interface [6–9].

In this regard, instead of an AFM layer, systems consisting of ferrimagnetic (FI) heavy rare earth (RE)-3*d* transition metal (TM) alloys provide further benefits as pinning layers since these alloys can exhibit large interfacial exchange interaction and zero moment at the compensation temperature T_{comp}. Below the compensation temperature, the heavy RE magnetization dominates, while above T_{comp}, the TM magnetization is the leading one. This behavior has some very interesting consequences when FI/FM [10–18], FI/FI [19–27] systems are considered. For instance let us assume that only one of the two FI layers is RE dominated; then in the ground state, there is an antiparallel alignment of the net magnetizations of each layer. However, when one layer is reversed against the other by an external field, this will create an interfacial domain wall (IDW) in order to minimize the cost of energy for the magnetic transition region between both layers [11,14]. If now the external field will be reduced coming from this configuration, at a certain field, the IDW annihilates, forcing the softer layer to rotate back so that the system can relax into its ground state. Due to the strong interfacial exchange coupling, the high amount of energy stored in the IDW gives rise to a large positive loop shift. Recently, exciting properties of a fully perpendicular FI/FI exchange coupled system consisting of $DyCo_5/Fe_{76}Gd_{24}$, where the $DyCo_5$ alloy has the role of the hard magnetic pinning layer, were reported [22]. It has been shown that the exchange coupling between the FI layers can be easily tuned by introducing a Ta spacer layer and that the shift of the hysteresis loop can be inverted, depending on the dominant moment (RE or TM). In other previous works, amorphous FI Tb-Fe thin films were coupled to somewhat softer FM [Co/Pt]-multilayers, forming a system with out-of-plane easy axis magnetization, which attracted much attention due to the occurrence of large interlayer exchange bias fields up to 20 kOe [13,14]. Similar results were recently reported for TbFeCo/[Co/Ni] heterostructures [28,29].

In this paper, the exchange interaction at the interface of TbFeCo/[Co/Pt] heterostructures was systematically varied by substitution of Fe by Co atoms in the amorphous TbFeCo layer for various Tb contents. Due to the higher exchange energy of Co-Co in comparison to Fe-Fe, a strong influence on the exchange interaction between the two layers is expected.

II. EXPERIMENTAL DETAILS

Single FI TbFeCo alloy films and coupled heterostructures with FM [Co/Pt] multilayers, both showing out-of-plane magnetic anisotropy, were prepared by dc magnetron co-sputtering at room temperature. The base pressure was below 4×10^{-8} mbar, and during the deposition, an Ar pressure of 1.5×10^{-3} mbar was used. The sample holder rotates during the deposition to ensure a uniform film composition. To protect the magnetic layers against oxidation and to improve film growth, a 5-nm-thick seed and capping layer of Pt was used. As substrate Si(001) wafers with a 100-nm-thick thermally oxidized SiO_2 layer were used, and in addition, films were also deposited on 200-nm-thick Si_3N_4 membranes for x-ray magnetic circular dichroism (XMCD) absorption

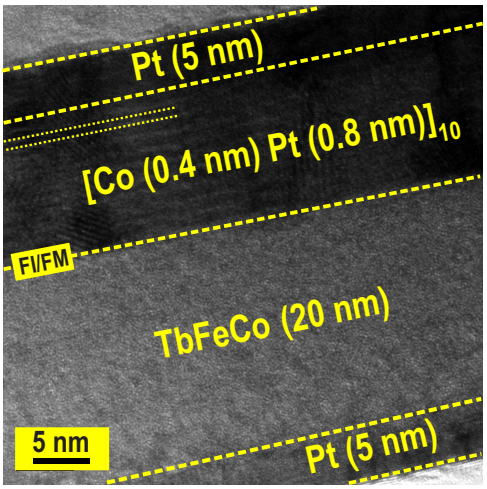

FIG. 1. Cross-section TEM image of a TbFeCo/$[Co(0.4\,nm)/Pt(0.8\,nm)]_{10}$ heterostructure embedded in Pt seed and capping layers.

measurements in transmission geometry to allow for sufficient transmission of soft x-rays.

In the first sample series, single 20-nm-thick TbFeCo alloy films were prepared choosing three different Tb contents ($x = 18$, 22, and 26 at.%) and varying for each of them the Co/Fe ratio in the following way, $Tb_x(Fe_{100-y}Co_y)_{100-x}$ with $y = 0$, 20, 40, 60, 80, and 100 at.%. However, throughout the text, the notation $Tb_xFe_{100-x-y}Co_y$ was used. All films show a strong out-of-plane magnetic anisotropy. In the second series, FI/FM heterostructures with out-of-plane magnetic anisotropy were prepared, combining the TbFeCo alloys of series 1 with a $[Co(0.4\,nm)/Pt(0.8\,nm)]_{10}$ multilayer. For this series, the influence of the Fe/Co ratio and the Tb content on the interfacial exchange coupling was systematically investigated.

The composition of the alloys and the thickness of each layer in the film structure were determined by Rutherford backscattering spectrometry (RBS). The structural properties were analyzed by transmission electron microscopy (TEM) imaging in top-view (not shown) and cross-section geometry and additionally by x-ray diffraction (XRD), revealing that all prepared TbFeCo alloys are amorphous. In Fig. 1, an exemplary cross-section image of a TbCoFe/$[Co/Pt]_{10}$ heterostructure is shown, revealing a smooth FI/FM interface with a roughness of about 1 nm. The integral magnetic properties were determined using a superconducting quantum interference device—vibrating sample magnetometer (SQUID-VSM). Full hysteresis loops were taken with a maximum external field of ± 70 kOe in a temperature range from 4 to 360 K, and additional minor loops were measured to extract the exchange bias field H_{EB}.

In a further study, the IDW formed in the TbFeCo/[Co/Pt] heterostructures was analyzed by element-specific XMCD absorption measurements in the temperature range from room temperature down to 10 K using the ALICE diffractometer installed at the PM3 beamline of the Helmholtz-Zentrum Berlin (HZB) [30]. The absorption experiments were performed at the Fe L_3-edge (708 eV), Co L_3-edge (778 eV), and Tb M_5-edge (1241 eV) for two samples of a further series, $Tb_{26}Fe_{74-y}Co_y$ ($y = 9$ and 30 at.%) coupled to $[Co(0.4\,nm)/Pt(0.8\,nm)]_{10}$ multilayers. In transmission geometry, the signals are proportional to the projection of the magnetization onto the photon propagation direction, therefore providing maximum sensitivity to perpendicular magnetized films. In addition, element specific hysteresis loops were measured up to a maximum external field of ± 6 kOe, which allowed determining the thickness of the IDW in the FI layer.

III. RESULTS AND DISCUSSION

Depending on the composition of the FI TbFeCo alloy, the net magnetization of the antiparallel aligned sublattices is either dominated by the Tb moments or by the Fe/Co moments. This behavior also depends on the temperature if the sample exhibits a compensation temperature. In Fig. 2(a), the magnetic properties of $Tb_{18}Fe_{82-y}Co_y$ thin films with varying Fe/Co ratio are presented. The saturation magnetization (M_S) and coercivity (H_C) are extracted from the easy axis hysteresis loops, which were measured by SQUID-VSM at different temperatures in out-of-plane geometry. The shapes of all hysteresis were rectangular. Additionally, hard axis hysteresis loops for in-plane geometry were measured as well to determine the anisotropy field (H_A) and to calculate the uniaxial magnetic anisotropy (K_U) by the following equation, $K_U = \frac{M_S \cdot H_A}{2} - 2 \cdot \pi \cdot M_S^2$, taking the shape anisotropy into account.

For this system, a decrease in M_S towards lower temperatures is observed, which is typical behavior for TM-dominated FI systems. As a result, a dominant increase of H_C at lower temperatures is observed. With increasing amount of Fe, the net magnetization raises as expected due to the larger Fe moment as compared to Co; however, the coercivity does not depend much on the Fe/Co ratio. The K_U values are reduced to lower temperatures, but interestingly, the anisotropy increases as more Fe substitutes Co.

For comparison, the magnetic properties of Tb-dominated $Tb_{26}Fe_{74-y}Co_y$ thin films are summarized in Fig. 2(b). For this case, M_S shows an increase towards lower temperatures and with increasing Co content, as expected for a RE-dominated system. For several compositions, a compensation temperature occurs within the available temperature range, where M_S vanishes. With increasing Fe content, the compensation temperature shifts to lower temperatures due to the larger magnetic moment compared to Co. As expected, H_C increases drastically close to the compensation temperature and towards lower temperatures. In contrast to the previous sample series with 18 at.% Tb, here the substitution of Co by Fe leads to higher coercive fields. The uniaxial anisotropy revealed a similar dependence as the magnetization, where for lower temperatures and smaller Co amount, K_U increases.

In the following, we will present the magnetic properties of the TbFeCo/[Co/Pt] heterostructures and discuss the influence of the Fe/Co ratio and Tb content on the reversal behavior and interface exchange coupling strength. In Fig. 3, temperature-dependent magnetic hysteresis (*M-H*) loops of $Tb_{18}Fe_{49}Co_{33}$/[Co/Pt] and $Tb_{26}Fe_{15}Co_{59}$/[Co/Pt] samples measured with the magnetic field applied out of the film plane are presented. Overall, the switching behavior

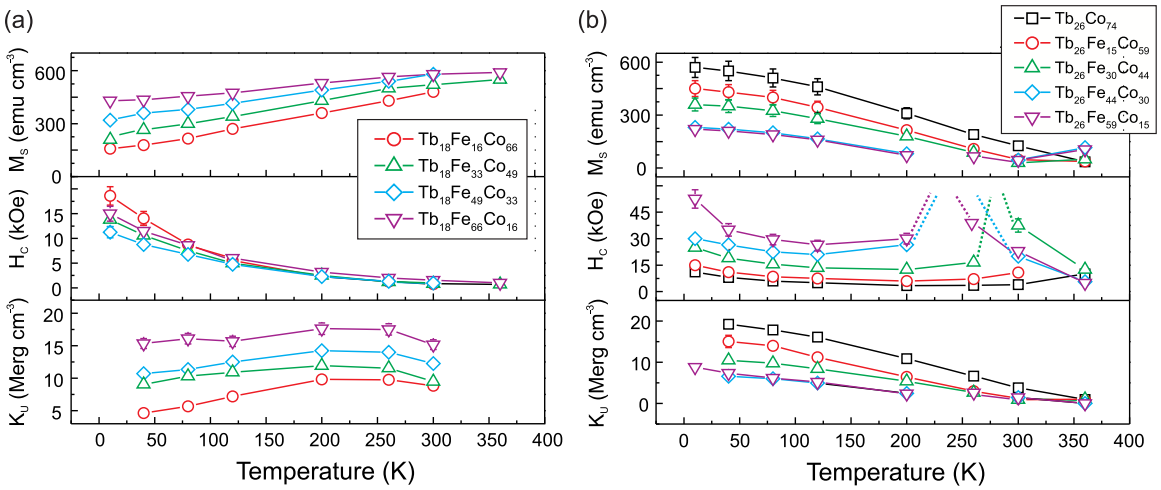

FIG. 2. Saturation magnetization M_S, coercivity H_C, and uniaxial magnetic anisotropy K_U of single $Tb_xFe_{100-x-y}Co_y$ alloy films as a function of temperature for two different Tb contents of (a) $x = 18$ at.% and (b) $x = 26$ at.%.

for the two samples is quite different, as expected due to the different dominant moments in the TbFeCo alloy. For the TM-dominated sample [Fig. 3(a)], the hysteresis shows a single step switching behavior with low coercivity for temperatures between 200 and 300 K. The Co/Fe moments of TbFeCo and [Co/Pt] are aligned parallel at remanence, which is the energetically preferred configuration. Here, K_U is much larger for the FI alloy (1.5×10^7 erg cm^{-3}) compared to the multilayer stack (3×10^6 erg cm^{-3}) over the whole temperature range, but due to the similar coercivities and strong exchange coupling of both layers, the bilayer reverses together. At temperatures below 200 K, the situation changes as now a clear two-step reversal process is observed. Here, M_S is getting smaller for the ferrimagnet, and H_C increases stronger than for the [Co/Pt] multilayer. For the latter, the K_U value is rather temperature independent. Starting from saturation and applying a negative reverse field, first, the softer [Co/Pt] layer reverses; consequently, a IDW will be formed [11,14,21]. By increasing the reverse field, this domain wall will be compressed and finally pushed further into the TbFeCo layer until the magnetization of the TbFeCo reverses in a single step in agreement with micromagnetic simulations [15,16].

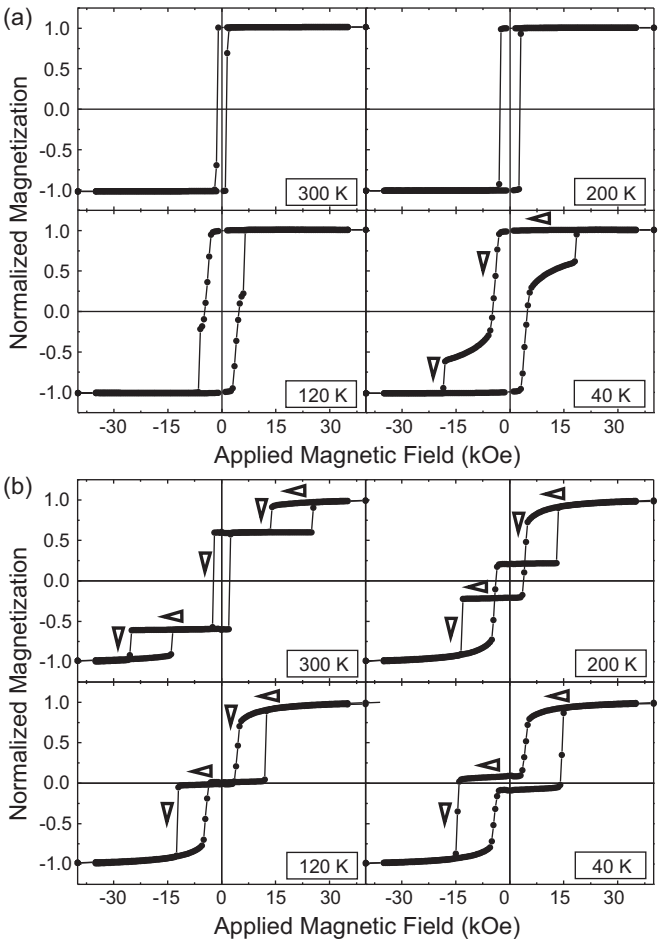

FIG. 3. Temperature-dependent out-of-plane (M-H) hysteresis loops of (a) $Tb_{18}Fe_{49}Co_{33}$ (20 nm)/[Co (0.4 nm)/Pt (0.8 nm)]$_{10}$ and (b) $Tb_{26}Fe_{15}Co_{59}$ (20 nm)/[Co (0.4 nm)/Pt (0.8 nm)]$_{10}$ heterostructures. Arrows mark the path of reversal.

In contrast, for a Tb-dominated sample, the net magnetization of $Tb_{26}Fe_{15}Co_{49}$ and [Co/Pt] is aligned antiparallel at remanence, while at saturation, an IDW is formed. By lowering the external field, the exchange coupling energy of the IDW will eventually overcome the Zeeman energy, and the energetically preferred antiparallel alignment of the sublattice magnetization will be realized before remanence. We detect this as the first reversal step, appearing in the hysteresis loops shown in Fig. 3(b). For temperatures below 200 K, the [Co/Pt] multilayer reverses first, and later at negative reverse fields, the magnetization of the TbFeCo layer reverses. For higher temperatures about room temperature, TbFeCo exhibits a lower K_U than the ferromagnet, and a more complex three-step reversal behavior can be observed. In this case, starting from positive saturation, the ferrimagnet reverses before remanence (annihilation of the IDW); then for a small negative reverse field, the coupled system reverses both its magnetization orientations, keeping the preferred antiparallel alignment until, at higher negative fields, the net magnetization of the TbFeCo layer is aligned to the external field nucleating an IDW.

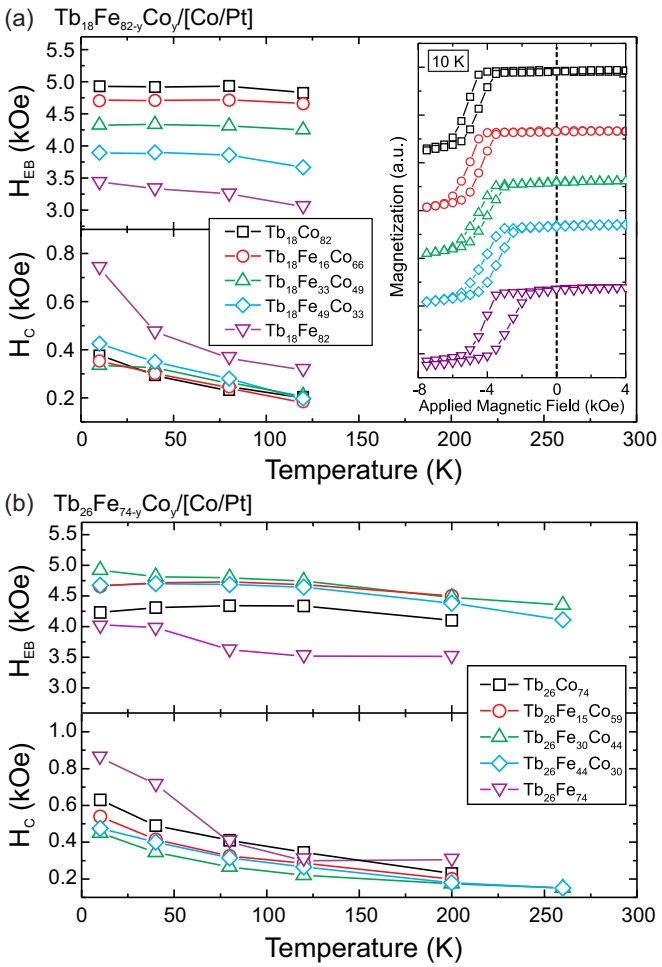

FIG. 4. Temperature dependence of the exchange bias field H_{EB} and coercivity H_C of the $[Co/Pt]_{10}$ multilayers as extracted from minor loops (see inset) from (a) $Tb_{18}Fe_{82-y}Co_y/[Co/Pt]_{10}$ (TM dominated) and (b) $Tb_{26}Fe_{74-y}Co_y/[Co/Pt]_{10}$ (Tb dominated) heterostructures.

In order to extract the exchange bias field H_{EB} of this coupled FI/FM system as function of temperature, the single reversal process of the magnetically softer [Co/Pt] multilayer was measured by minor loops after cooling down the samples from room temperature in +70 kOe. In this case, the applied magnetic field has to be lower than the coercivity of the hard magnetic TbFeCo layer, acting as the pinning layer [14]. Please note that, for Tb (Fe/Co)-dominated FI alloys, a positive (negative) shift is obtained starting from positive saturation. Prerequisite for extracting H_{EB} is a two-step switching behavior of the full hysteresis loop; thus, the temperature range where it takes place is limited. Figure 4(a) shows H_{EB} and corresponding H_C values of the [Co/Pt] layer when coupled to TM-dominated FI alloy films. In this case, during the minor loop reversal of the [Co/Pt] layer shown in the inset of Fig. 4(a), an IDW is formed and annihilated. Values are only obtained for temperatures below 130 K. The exchange bias field of the system shows a slight increase towards lower temperatures but reveals a strong influence on the Co content of the ternary alloy: the larger the Co content, the higher the H_{EB}. Looking at the two extreme cases, from the binary TbFe alloy to TbCo,

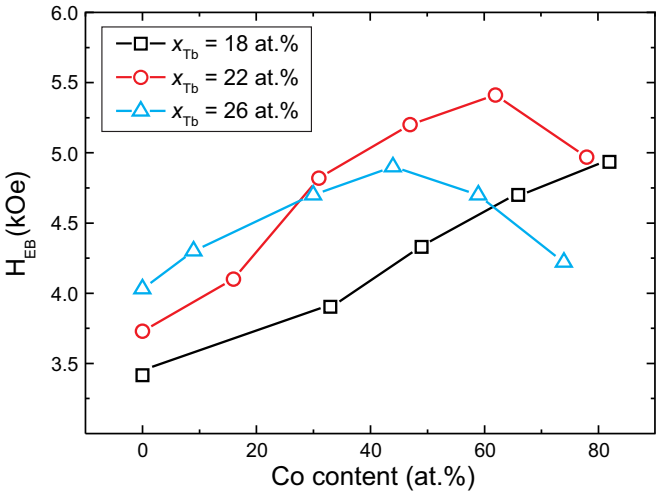

FIG. 5. Exchange bias field H_{EB} at 10 K as function of Co content in $Tb_xFe_{100-x-y}Co_y/[Co/Pt]_{10}$ heterostructures for three different Tb contents.

an increase in H_{EB} of about 1.5 kOe is obtained. In contrast, for heterostructures consisting of Tb-dominated alloy films, no linear dependence of H_{EB} with increasing Co content is observed [Fig. 4(b)]. Instead, H_{EB} reveals a maximum value of about 5 kOe at 10 K for the $Tb_{26}Fe_{30}Co_{44}/[Co/Pt]$ heterostructure. In addition, a correlation to the coercivity is apparent in the two systems: the larger the H_{EB}, the smaller the H_C.

The dependence of H_{EB} (absolute values) obtained at 10 K on the Fe-Co ratio for three different Tb contents of the FI alloy is summarized in Fig. 5. As the exchange coupling between Co-Co pairs is the strongest ($J_{Co\text{-}Co} > J_{Co\text{-}Fe} > J_{Fe\text{-}Fe}$), a linear increase in H_{EB} with increasing Co content was expected. However, as shown in Fig. 5, with increasing Tb content ($x =$ 22 and 26 at.%), the curves show a maximum. This maximum shifts to lower Co concentration with increasing Tb content in the ternary alloy. In our FI/FM system, the exchange bias field H_{EB} depends on the interfacial exchange energy density J_E, the thickness of the FM layer t_{FM}, and its saturation magnetization $M_{S,FM}$, as given by the following equation [26]:

$$H_{EB} = -\frac{J_E}{M_{S,FM}t_{FM}} = -\frac{\sigma_{IDW}}{2M_{S,FM}t_{FM}} = -\frac{\pi\sqrt{A_{eff}\cdot K_{eff}}}{M_{S,FM}t_{FM}}$$

This formula can also be expressed in terms of effective exchange stiffness A_{eff} and magnetic anisotropy K_{eff} or by the IDW energy σ_{IDW}. As we have used for all heterostructures the same FM [Co/Pt] layer, the changes observed in H_{EB} depend solely on the magnetic properties of the TbFeCo alloy [31]. As we know from our previous results of a TM-dominated alloy with $x_{Tb} = 18$ at.% shown in Fig. 2(a), at a certain temperature the magnetic anisotropy decreases with increasing Co content. If the magnetic anisotropy would play the dominant role in these systems, H_{EB} should decrease as more Co substitutes Fe, but the opposite behavior is observed: H_{EB} increases linearly with Co content [Fig. 5]. Thus, we can conclude that the key parameter is given by the exchange stiffness A, which is directly correlated to the interatomic exchange constant J. As the interatomic magnetic coupling of Co atoms

$J_{\text{Co-Co}}$ present at the interface between [Co/Pt] and TbFeCo is largest, alloys with higher amount of Co should exhibit higher values for the exchange bias field, which is in agreement to the results observed for the sample series with $x_{\text{Tb}} = 18$ at.%. However, with increasing amount of Tb, a maximum of H_{EB} in dependence of the Co content was observed. This rather unexpected behavior can be explained by taking into account the variation of exchange energies of Co-Co and Fe-Fe pairs with changing RE content as reported by Hansen *et al.* [32]. For instance, in GdFeCo alloys, the exchange energy for Co-Co pairs decreases for higher Gd content, while the exchange energy of Fe-Fe pairs increases. Assuming a similar behavior for TbFeCo alloys and neglecting variations in the exchange energy of Tb-TM pairs as well as at the interface, the maximum of H_{EB} should shift to lower Co concentration with increasing Tb amount, which is indeed observed (see Fig. 5). This correlation of the interface coupling strength, depending on the RE element in amorphous FI alloys, can also explain the increasing H_{EB} for higher Tb content for coupled heterostructures with binary Tb-Fe alloys [14]. With increasing Tb content in the alloy, the stiffness increases, which results in a higher exchange bias field.

In a further study, the thickness of the IDW formed during the reversal process of the [Co/Pt] multilayer was analyzed by element-specific XMCD measurements for two Tb-dominated samples, $Tb_{26}Fe_{44}Co_{30}/[Co/Pt]_{10}$ and $Tb_{26}Fe_{65}Co_9/[Co/Pt]_{10}$, prepared on Si_3N_4 membranes. The temperature was varied in a broad range (10–360 K), and the maximum external field of ±6 kOe was sufficient to switch the [Co/Pt] multilayer and to form an IDW.

Figure 6 shows element-specific magnetic hysteresis loops based on XMCD contrast taken at the Co, Fe, and Tb absorption edges at 120 K, revealing opposite sign due to the antiparallel coupling of the magnetic moments of Fe/Co and Tb. In this case, the Fe and Tb loops disclose exclusively the partially reversed part of the FI layer, which occurs during the reversal of the [Co/Pt] multilayer. Thus, these loops show the contribution of Fe and Tb of the created IDW in the FI layer,

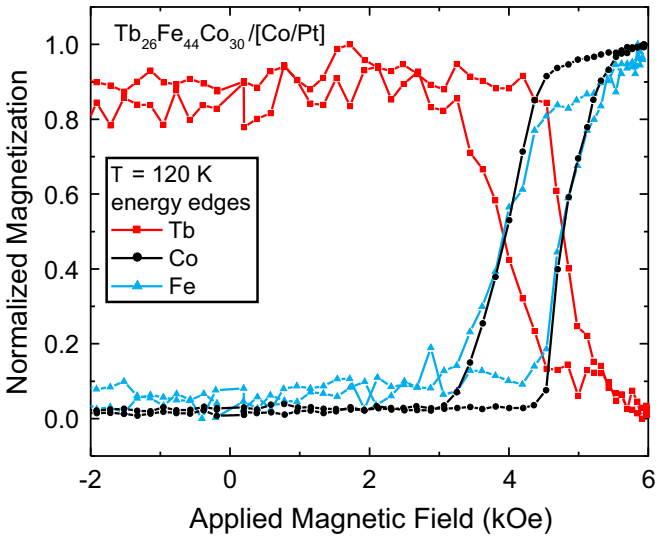

FIG. 6. Element-specific XMCD minor loops of a $Tb_{26}Fe_{44}Co_{30}/[Co/Pt]_{10}$ heterostructure measured at 120 K.

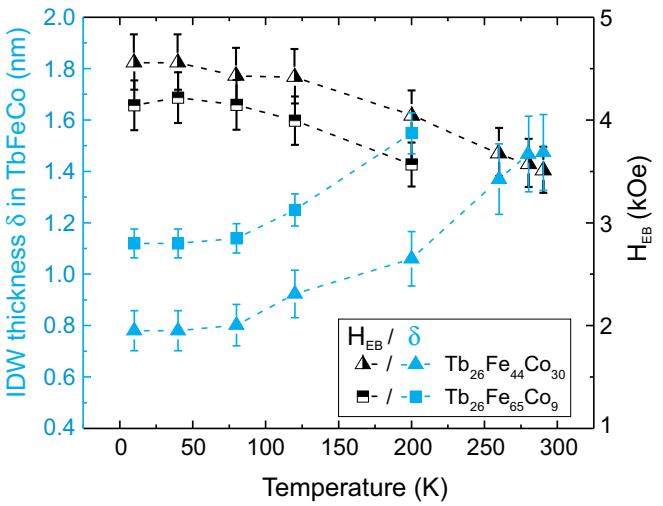

FIG. 7. Temperature dependence of the thickness of the IDW located in TbFeCo and the interfacial exchange bias field H_{EB} for $Tb_{26}Fe_{65}Co_9/[Co/Pt]_{10}$ and $Tb_{26}Fe_{44}Co_{30}/[Co/Pt]_{10}$ heterostructures as measured by XMCD absorption at the Fe edge.

while the remaining part of the ferrimagnet acts as pinning layer. This IDW also exists in the [Co/Pt] multilayer; however, its contribution cannot be analyzed by the Co loop as it mainly represents the reversal of the full [Co/Pt] multilayer.

The thickness of the IDW of the FI layer was estimated by comparing the recorded XMCD signal taken at the Fe L_3 edge of the fully reversed 20-nm-thick TbFeCo layer, which is detectable at higher temperatures, with the XMCD signal coming from the IDW. This approach is based on the different intensities $I^{(+/-)}$ detected in positive and negative field direction along the photon propagation direction, which are associated with different absorption coefficients $\mu^{(+/-)}$. The latter depend on the thickness t of the absorbing material given by $I^{(+/-)} = I_0 e^{-t\mu(+/-)}$. Based on that, the thickness of the IDW in the FI layer can be estimated. The extracted values are presented in Fig. 7 as a function of temperature. In addition, the temperature behavior of H_{EB} is included in the graph for comparison. As expected, a larger H_{EB} is observed for the alloy with higher Co content (see also Fig. 5), which increases towards lower temperatures for both samples. In contrast, the thickness of the IDW shows the opposite behavior: it becomes thinner for decreasing temperature and for higher Co content. Hence, there is a clear relationship between the IDW thickness in the ferrimagnet and the exchange coupling field: the thinner the domain wall, the larger the H_{EB}.

The increase of H_{EB} towards lower temperatures needs to be associated with an increase in domain wall energy at the interface, which depends on the parameters K_{eff} and A_{eff}. For the two samples, the magnetic anisotropy of the FI layer is increasing at low temperatures [see Fig. 3(b)]. In addition, an increase of A_{eff} towards lower temperatures is expected as well [33–35]. Furthermore, higher exchange stiffness is expected for the sample with the larger Co content. Therefore, the cost of a domain wall in the FI is higher for the $Tb_{26}Fe_{44}Co_{30}$ sample. As the [Co/Pt] multilayer exhibits smaller anisotropy values, we expect that most of the domain wall is located in the [Co/Pt] multilayer, resulting in a thinning

of the domain wall in the ferrimagnet with increasing domain wall energy density in the FI layer. This conclusion is well supported by earlier results reported by Watson *et al.* [12] using polarized neutron reflectometry, revealing that the IDW present in TbFeCo/[Co/Pd] heterostructures is mainly located in the [Co/Pd] multilayer.

IV. CONCLUSION

In conclusion, the interfacial exchange coupling of TbFeCo/[Co/Pt] heterostructures was systematically studied by varying the composition of the amorphous TbFeCo layers, which supports a tunable composition in a wide range. In particular, the dependence of the exchange bias field on the Co-Fe ratio for different Tb contents using minor loop studies of the [Co/Pt] multilayer was investigated. The benefit of using heavy RE-TM alloys as pinning layer is the tunable magnetic properties that depend strongly on temperature and composition. In this regard, due to the higher exchange energy of Co-Co in comparison to Fe-Fe, a strong influence on the exchange interaction between the two layers is expected. However, while for Fe/Co-dominated TbFeCo alloys, the exchange bias field increases rather linearly with Co content, a maximum is observed for Tb-dominated systems. Interestingly, this maximum shifts to lower Co content as more Tb is present in the alloy. By looking at the relevant magnetic parameters obtained from TbFeCo single layers, it turned out that this behavior is mainly given by the variation of the exchange stiffness. In a further study, XMCD absorption measurements at the Fe L_3 edge were employed to follow the nucleation and annihilation process of the IDW in Tb-dominated TbFeCo layers during [Co/Pt] reversal. From these measurements, the IDW thickness was estimated and correlated to the underlying magnetic properties. Here, the following relationship was found: the exchange bias field increases with the exchange stiffness and magnetic anisotropy of the alloy, which results in a thinning of the IDW in the FI TbFeCo layer.

ACKNOWLEDGMENT

The authors thank the HZB for allocation of beam time at Beamline PM3 (ALICE) and R. Wilhelm (HZ Dresden-Rossendorf) for RBS measurements. The financial support provided by the Deutsche Forschungsgemeinschaft (Grant No. AL 618/21-1) is gratefully acknowledged.

[1] W. H. Meiklejohn and C. P. Bean, Phys. Rev. **102**, 1413 (1956).
[2] I. L. Prejbeanu, S. Bandiera, J. Alvarez-Hérault, R. Sousa, B. Dieny, and J. P. Nozières, J. Phys. D. Appl. Phys. **46**, 074002 (2013).
[3] S. Roy, M. R. Fitzsimmons, S. Park, M. Dorn, O. Petracic, I. V. Roshchin, Z. P. Li, X. Batlle, R. Morales, A. Misra, X. Zhang, K. Chesnel, J. B. Kortright, S. K. Sinha, and I. K. Schuller, Phys. Rev. Lett. **95**, 047201 (2005).
[4] F. Radu and H. Zabel, Springer Tracts Mod. Phys. **227**, 97 (2008).
[5] K. O'Grady, L. Fernandez-Outon, and G. Vallejo-Fernandez, J. Magn. Magn. Mater. **322**, 883 (2010).
[6] I. Schmid, M. A. Marioni, P. Kappenberger, S. Romer, M. Parlinska-Wojtan, H. J. Hug, O. Hellwig, M. J. Carey, and E. E. Fullerton, Phys. Rev. Lett. **105**, 197201 (2010).
[7] H. Ohldag, T. J. Regan, J. Stöhr, A. Scholl, F. Nolting, J. Lüning, C. Stamm, S. Anders, and R. L. White, Phys. Rev. Lett. **87**, 247201 (2001).
[8] H. Ohldag, A. Scholl, F. Nolting, E. Arenholz, S. Maat, A. T. Young, M. Carey, and J. Stöhr, Phys. Rev. Lett. **91**, 017203 (2003).
[9] J. Wu, J. S. Park, W. Kim, E. Arenholz, M. Liberati, A. Scholl, Y. Z. Wu, C. Hwang, and Z. Q. Qiu, Phys. Rev. Lett. **104**, 217204 (2010).
[10] F. Canet, S. Mangin, C. Bellouard, and M. Piecuch, Europhys. Lett. **52**, 594 (2000).
[11] S. Mangin, T. Hauet, P. Fischer, D. H. Kim, J. B. Kortright, K. Chesnel, E. Arenholz, and E. E. Fullerton, Phys. Rev. B **78**, 024424 (2008).
[12] M. Watson, T. Hauet, J. A. Borchers, S. Mangin, and E. E. Fullerton, Appl. Phys. Lett. **92**, 202507 (2008).
[13] S. Romer, M. A. Marioni, K. Thorwarth, N. R. Joshi, C. E. Corticelli, H. J. Hug, S. Oezer, M. Parlinska-Wojtan, and H. Rohrmann, Appl. Phys. Lett. **101**, 222404 (2012).
[14] C. Schubert, B. Hebler, H. Schletter, A. Liebig, M. Daniel, R. Abrudan, F. Radu, and M. Albrecht, Phys. Rev. B **87**, 054415 (2013).
[15] H. Oezelt, A. Kovacs, P. Wohlhüter, E. Kirk, D. Nissen, P. Matthes, L. J. Heyderman, M. Albrecht, and T. Schrefl, J. Appl. Phys. **117**, 17E501 (2015).
[16] H. Oezelt, A. Kovacs, F. Reichel, J. Fischbacher, S. Bance, M. Gusenbauer, C. Schubert, M. Albrecht, and T. Schrefl, J. Magn. Magn. Mater. **381**, 28 (2015).
[17] M. Patra, M. Thakur, S. Majumdar, and S. Giri, J. Phys.: Condens. Matter **21**, 236004 (2009).
[18] M. Ungureanu, K. Dumesnil, C. Dufour, N. Gonzalez, F. Wilhelm, A. Smekhova, and A. Rogalev, Phys. Rev. B **82**, 174421 (2010).
[19] S. Mangin, F. Montaigne, and A. Schuhl, Phys. Rev. B **68**, 140404 (2003).
[20] T. Hauet, J. A. Borchers, P. Mangin, Y. Henry, and S. Mangin, Phys. Rev. Lett. **96**, 067207 (2006).
[21] T. Hauet, S. Mangin, F. Montaigne, J. A. Borchers, and Y. Henry, Appl. Phys. Lett. **91**, 022505 (2007).
[22] F. Radu, R. Abrudan, I. Radu, D. Schmitz, and H. Zabel, Nat. Commun. **3**, 715 (2012).
[23] C.-C. Lin, C.-H. Lai, R.-F. Jiang, and H.-P. D. Shieh, J. Appl. Phys. **93**, 6832 (2003).
[24] S. Mangin, T. Hauet, Y. Henry, F. Montaigne, and E. E. Fullerton, Phys. Rev. B **74**, 024414 (2006).
[25] T. Hauet, F. Montaigne, M. Hehn, Y. Henry, and S. Mangin, Phys. Rev. B **79**, 224435 (2009).
[26] T. Tokunaga, M. Taguchi, T. Fukami, and K. Tsutsumi, J. Appl. Phys. **67**, 4417 (1990).
[27] K. Chen, D. Lott, F. Radu, F. Choueikani, E. Otero, and P. Ohresser, Scientific Reports **5**, 18377 (2015).

[28] M. H. Tang, Z. Zhang, S. Y. Tian, J. Wang, B. Ma, and Q. Y. Jin, Sci. Rep. **5**, 10863 (2015).
[29] M. H. Tang, Z. Zhang, Y. Zu, B. Ma, and Q. Y. Jin, Nano-Micro Lett. **6**, 359 (2014).
[30] R. Abrudan, F. Bruessing, R. Salikhov, J. Meermann, I. Radu, H. Ryll, F. Radu, and H. Zabel, Rev. Sci. Instrum. **86**, 063902 (2015).
[31] T. Wu, H. Fu, R. A. Hajjar, T. Suzuki, and M. Mansipur, J. Appl. Phys. **73**, 1368 (1993).
[32] P. Hansen, C. Claussen, G. Much, M. Rosenkranz, and K. Witter, J. Appl. Phys. **66**, 756 (1989).
[33] T. Nakamura and M. Bloch, Phys. Rev. **132**, 2528 (1963).
[34] U. Axitia, D. Hinzke, O. Chubykalo-Fesenko, U. Nowak, H. Kachkachi, O. N. Mryasov, R. F. Evans, and R. W. Chantrell, Phys. Rev. B **82**, 134440 (2010).
[35] D. Raasch, J. Reck, C. Mathieu, and B. Hillebrands, J. Appl. Phys. **76**, 1145 (1994).